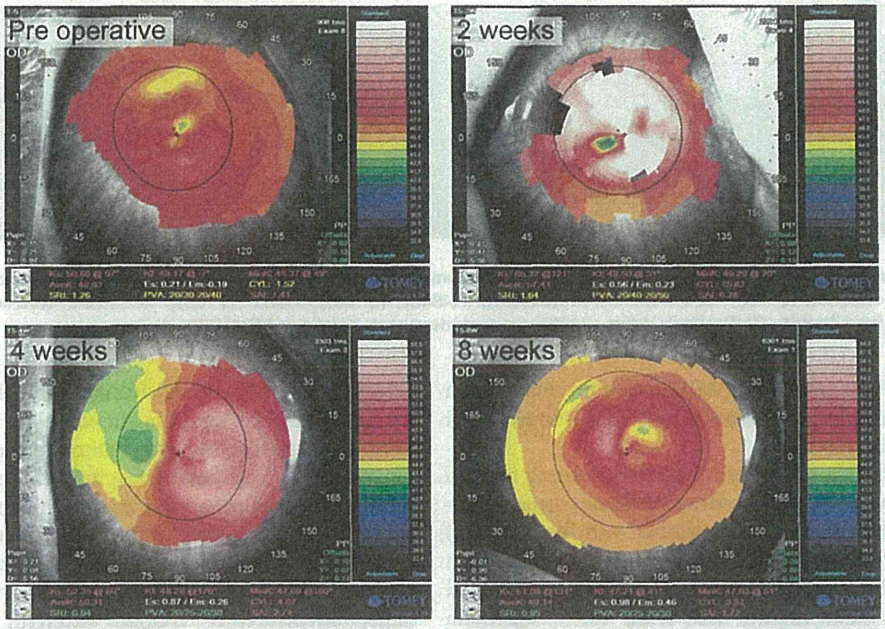

Figure 5. Change in corneal topography following implantation of BIOSHEETs into rabbit cornea

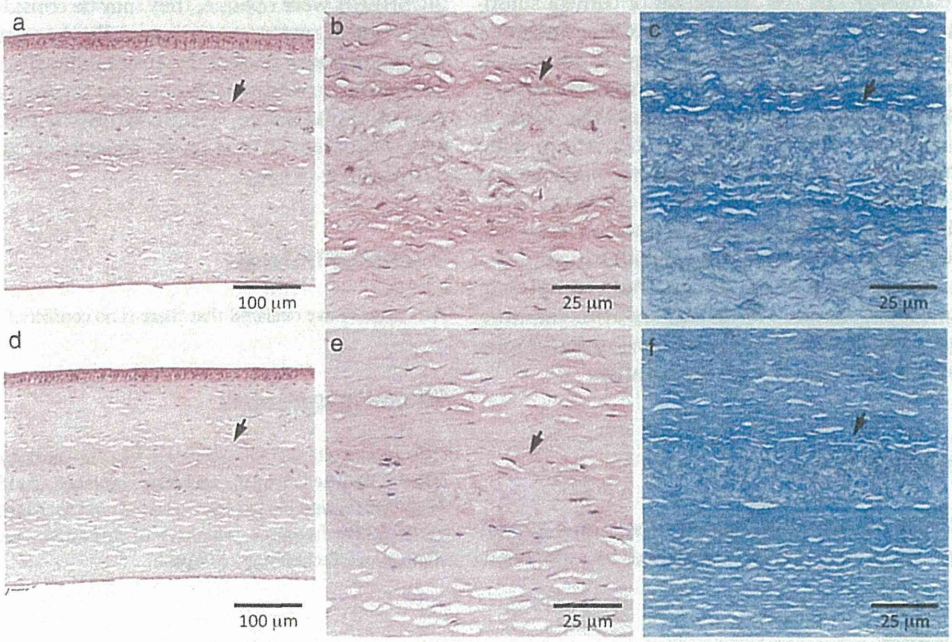

Figure 6. Histological section of rabbit corneas implanted with BIOSHEETs at 4 weeks (a–c) and 8 weeks postoperatively (d–f). Black arrows indicate the anterior surface of the implanted BIOSHEET. (a,d) Low-magnification images and (b,e) high-magnification images of haematoxylin and eosin-stained sections. (c,f) High-magnification images of Masson trichrome-stained sections

However, at 4 weeks postoperatively, the corneal thickness and the transparency score had decreased. The increase in corneal thickness and corneal opacity observed immediately after implantation may have been caused by the swelling of the BIOSHEETs, and the subsequent decrease in corneal thickness and recovery of transparency may be attributed to dehydration of the BIOSHEETs. At 8 weeks postoperatively, the transparency score had improved ($p = 0.04$), the corneal thickness had not changed and the histological arrangement and orientation of collagen lamellae of implanted BIOSHEETs became homogeneous relative to the sheets observed at 4 weeks. These results suggest that recovery of corneal transparency from 4 weeks to 8 weeks results from structural changes such as remodelling of the BIOSHEETs without degradation, thereby altering the light-scattering properties. The

DOI: 10.1002/term

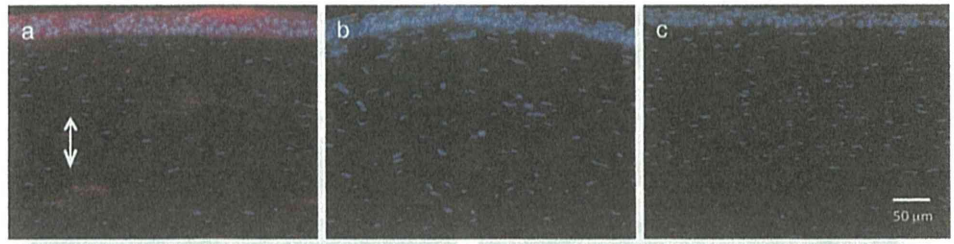

Figure 7. Immunohistological section of rabbit corneas implanted with BIOSHEETs at 8 weeks. Fluorescent microscopic images stained with vimentin (a, red), alpha smooth muscle actin (α-SMA) (b, red), RAM11 (c, red). Cell nuclei were stained with 4′,6-diamidino-2-phenylindole (DAPI, blue). White double arrow indicates the region of BIOSHEET implantation

histological structure of BIOSHEETs before implantation showed a lamellar arrangement of collagen fibres, which may facilitate remodelling.

The BIOSHEETs implanted into rabbit corneas showed high biocompatibility and tendency to restore corneal transparency. These results are compatible with the results of other studies of biosynthetic corneal implant materials such as recombinant human collagen hydrogels, decellularized corneas and rabbit dermis (Liu *et al.*, 2007; Fagerholm *et al.*, 2009; Merrett *et al.*, 2009; Duncan *et al.*, 2010; Tanaka *et al.*, 2011). Recent developments in tissue engineering technology and the production of corneal substitutes may be used to address the worldwide shortage of acceptable donor corneas. However, many of the present approaches require costly equipment and complex methodology. Globally, corneal opacity is an important cause of blindness or severe visual impairment that affects more than 10 million people, most of whom live in developing countries (Whitcher *et al.*, 2001, 2002; Schwartz *et al.*, 1997). Corneal transplantation in these areas has many limitations, including a lack of eye banking infrastructure and excessive cost (Feilmeier *et al.*, 2010). Thus, for development of prosthetic tissues, our in-body tissue architecture technology is simple, safe and cost-effective, making it particularly advantageous in developing countries.

5. Conclusion

BIOSHEETs fabricated using in-body tissue architecture technology were successfully implanted as allogeneic substitutes in the corneal stroma in a rabbit model with biological stability and biocompatibility. However, long-term biocompatibility, mechanical strength and graft innervation are also necessary for an ideal corneal scaffold. Mechanical properties are also important for tissue engineering materials. Studies to evaluate the mechanical properties of BIOSHEETs are therefore in progress. Further studies will address the long-term biocompatibility, ultrastructural changes, strength, reinnervation, and functionality of implanted BIOSHEETs in both normal and damaged cornea. Although the original BIOSHEETs were opaque, they may be considered a practical corneal replacement, especially in treatment for visual impairment caused by stromal opacity, because the transparency of the cornea increased progressively with time of implantation. The BIOSHEET is the first corneal material based on the novel concept of conversion to transparency *in situ*.

Conflict of interest

The authors have declared that there is no conflict of interest.

Acknowledgements

The authors thank Manami Sone for her participation and Dr Takeshi Moriwaki for his technical assistance in this study. This study was funded in part by a grant-in-aid for Scientific Research (B23360374) from the Ministry of Education, Culture, Sports, Science and Technology of Japan.

References

Antonogiannakis E, Yiannakopoulos CK, Hiotis I, *et al.* 2005; Arthroscopic anterior cruciate ligament reconstruction using quadriceps tendon autograft and bioabsorbable cross-pin fixation. *Arthroscopy* **21**: 894.e1–e5.

Bray LJ, George KA, Ainscough SL, *et al.* 2011; Human corneal epithelial equivalents constructed on *Bombyx mori* silk fibroin membranes. *Biomaterials* **32**: 5086–5091.

Builles N, Justin V, André V, *et al.* 2007; Reconstructed corneas: effect of three-dimensional culture, epithelium, and tetracycline hydrochloride on newly synthesized extracellular matrix. *Cornea* **26**: 1239–1248.

Carey JL, Dunn WR, Dahm DL, *et al.* 2009; A systematic review of anterior cruciate ligament reconstruction with autograft compared with allograft. *J Bone Joint Surg Am* **91**: 2242–2250.

Chen J, Li Q, Xu J, *et al.* 2005; Study on biocompatibility of complexes of collagen–chitosan–sodium hyaluronate and cornea. *Artif Organs* **29**: 104–113.

Chen W, Lin Y, Zhang X, *et al.* 2010; Comparison of fresh corneal tissue versus glycerin-cryopreserved corneal tissue in deep anterior lamellar keratoplasty. *Invest Ophthalmol Vis Sci* **51**: 775–781.

Chong EM, Dana MR. 2008; Graft failure IV. Immunologic mechanisms of corneal transplant rejection. *Int Ophthalmol* **28**: 209–222.

Crawford GJ, Constable IJ, Chirila TV, *et al.* 1993; Vijayasekaran S, Thompson DE. Tissue interaction with hydrogel sponges implanted in the rabbit cornea. *Cornea* **12**: 348–357.

Doane MG, Dohlman CH, Bearse G. 1996; Fabrication of a keratoprosthesis. *Cornea* **15**: 179–184.

Duncan TJ, Tanaka Y, Shi D, *et al.* 2010; Flow-manipulated, crosslinked collagen gels for use as corneal equivalents. *Biomaterials* **31**: 8996–9005.

Fagerholm P, Lagali NS, Carlsson DJ, *et al.* 2009; Corneal regeneration following implantation of a biomimetic tissue-engineered substitute. *Clin Transl Sci* **2**: 162–164.

Fagerholm P, Lagali NS, Merrett K, *et al.* 2010; A biosynthetic alternative to human donor tissue for inducing corneal regeneration: 24-month follow-up of a phase 1 clinical study. *Sci Transl Med* **2**: 46–61.

Feinberg AW. 2012; Engineered tissue grafts: opportunities and challenges in regenerative medicine. *WIREs Syst Biol Med* **4**: 207–220.

Feilmeier MR, Tabin GC, Williams L, *et al.* 2010; The use of glycerol-preserved corneas in the developing world. *Middle East Afr J Ophthalmol* **17**: 38–43.

Hassell JR, Birk DE. 2010; The molecular basis of corneal transparency. *Exp Eye Res* **91**: 326–335.

Hayashida K, Kanda K, Yaku H, *et al.* 2007; Development of an *in vivo* tissue-engineered, autologous heart valve (the biovalve): preparation of a prototype model. *J Thorac Cardiovasc Surg* **134**: 152–159.

Jackson DW, Simon TM. 2002; Donor cell survival and repopulation after intra-articular transplantation of tendon and ligament allografts. *Microsc Res Tech* **58**: 25–33.

King JH Jr, McTigeu JW, Meryman HT. 1962; A simple method of preservation of corneas for lamellar keratoplasty. *Am J Ophthalmol* **53**: 445–449.

Knupp C, Pinali C, Lewis PN, *et al.* 2009; The architecture of the cornea and structural basis of its transparency. *Adv Protein Chem Struct Biol* **78**: 25–49.

Lee SD, Hsiue GH, Kao CY, *et al.* 1996; Artificial cornea: surface modification of silicone rubber membrane by graft polymerization of pHEMA via glow discharge. *Biomaterials* **17**: 587–595.

Li J, Shi S, Zhang X, *et al.* 2012; Comparison of different methods of glycerol preservation for deep anterior lamellar keratoplasty eligible corneas. *Invest Ophthalmol Vis Sci* **53**: 5675–5685.

Liu L, Kuffová L, Griffith M, 2007; Immunological responses in mice to full-thickness corneal grafts engineered from porcine collagen. *Biomaterials* **28**: 3807–3814.

Merrett K, Liu W, Mitra D, *et al.* 2009; Synthetic neoglycopolymer-recombinant human collagen hybrids as biomimetic crosslinking agents in corneal tissue engineering. *Biomaterials* **30**: 5403–5408.

Nakayama Y, Ishibashi-Ueda H, Takamizawa K. 2004; *In vivo* tissue-engineered small-caliber arterial graft prosthesis consisting of autologous tissue (biotube). *Cell Transplant* **13**: 439–449.

National Institutes of Health. 1996; Guide for the Care and Use of Laboratory Animals. NIH Publication No. 85–23, revised 1996. NIH, Bethesda, MD.

Quantock AJ, Kratz-Owens KL, Leonard DW, *et al.* 1994; Remodelling of the corneal stroma after lamellar keratoplasty: a synchrotron X-ray study. *Cornea* **13**: 20–27.

Robert L, Legeais JM, Robert AM. *et al.* 2001; Corneal collagens. *Pathol Biol (Paris)* **49**: 353–363.

Schwartz EC, Huss R, Hopkins A, *et al.* 1997; Blindness and visual impairment in a region endemic for onchocerciasis in the Central African Republic. *Br J Ophthalmol* **81**: 443–447.

Sharma A, Gupta P, Narang S, *et al.* 2001; Clear tectonic penetrating graft using glycerine-preserved donor cornea. *Eye (Lond)* **15**: 345–347.

Streilein JW, Yamada J, Dana MR, *et al.* 1999; Ksander BR. Anterior chamber-associated immune deviation, ocular immune privilege, and orthotopic corneal allografts. *Transplant Proc* **31**: 1472–1475.

Tanaka Y, Shi D, Kubota A, *et al.* 2011; Irreversible optical clearing of rabbit dermis for autogenic corneal stroma transplantation. *Biomaterials* **32**: 6764–6772.

Vijayasekaran S, Hicks CR, Chirila TV, *et al.* 1997; Histologic evaluation during healing of hydrogel core-and-skirt keratoprostheses in the rabbit eye. *Cornea* **16**: 352–359.

de Vries Reilingh TS, Bodegom ME, van Goor H, *et al.* 2007; Autologous tissue repair of large abdominal wall defects. *Br J Surg* **94**: 791–803.

Watanabe T, Kanda K, Yamanami M, *et al.* 2011; Long-term animal implantation study of biotube-autologous small-caliber vascular graft fabricated by in-body tissue architecture. *J Biomed Mater Res B Appl Biomater* **98**: 120–126.

Whitcher JP, Srinivasan M, Upadhyay MP. 2001; Corneal blindness: a global perspective. *Bull World Health Org* **79**: 214–221.

Whitcher JP, Srinivasan M, Upadhyay MP. 2002; Prevention of corneal ulceration in the developing world. *Int Ophthalmol Clin* **42**: 71–77.

Williams KA, Coster DJ. 2007; The immunobiology of corneal transplantation. *Transplantation* **84**: 806–813.

Xiao J, Duan H, Liu Z, *et al.* 2011; Construction of the recellularized corneal stroma using porous acellular corneal scaffold. *Biomaterials* **32**: 6962–6971.

Yamanami M, Yahata Y, Uechi M, *et al.* 2010; Development of a completely autologous valved conduit with the sinus of Valsalva using in-body tissue architecture technology: a pilot study in pulmonary valve replacement in a beagle model. *Circulation* **122**(11 Suppl): 100–106.

Yoeruek E, Bayyoud T, Maurus C, *et al.* 2011; Reconstruction of corneal stroma with decellularized porcine xenografts in a rabbit model. *Acta Ophthalmol* **90**: e206–e210.

J Artif Organs (2015) 18:40–47
DOI 10.1007/s10047-014-0793-x

ORIGINAL ARTICLE — Artificial Valve

In situ observation and enhancement of leaflet tissue formation in bioprosthetic "biovalve"

Marina Funayama · Yoshiaki Takewa · Tomonori Oie · Yuichi Matsui · Eisuke Tatsumi · Yasuhide Nakayama

Received: 11 September 2014 / Accepted: 27 September 2014 / Published online: 5 November 2014

Abstract Biovalves, autologous tri-leaflet valved conduits, are formed in the subcutaneous spaces of animals. The valves are formed using molds encapsulated with autologous connective tissues. However, tissue migration into the small apertures in the molds for leaflet formation is generally slower than that for conduit formation around the molds. In this study, the formation of the leaflet tissues was directly and non-invasively observed using a wireless capsule endoscope. The molds were assembled from 6 parts, one of which was impregnated with the endoscope, and embedded into subcutaneous pouches in goats ($n = 30$). Tissue ingrowth into the apertures gradually occurred from the edges of the leaflet parts. Tissue formation was accompanied by capillary formation. At 63.1 ± 17.1 days after embedding, the apertures were completely replaced with autologous connective tissue, forming the leaflet tissues. Leaflet formation was enhanced by including fat tissue (46.7 ± 4.2 days) or blood (41.1 ± 6.9 days) in the apertures before embedding. The creation of slit openings, in conjunction with addition of blood to the apertures, further enhanced leaflet formation (37.0 ± 2.8 days). Since leaflet formation could be observed endoscopically, the appropriate embedding period for complete biovalve formation could be determined.

Keywords In vivo tissue engineering · Biovalve · Heart valve · Tissue formation · Endoscope

M. Funayama · T. Oie · Y. Matsui · Y. Nakayama (✉)
Division of Medical Engineering and Materials, National Cerebral and Cardiovascular Center Research Institute, 5-7-1 Fujishiro-dai, Suita, Osaka 565-8565, Japan
e-mail: nakayama@ri.ncvc.go.jp; ny@ncvc.go.jp

M. Funayama
College of Bioresource Sciences, Nihon University, Fujisawa, Kanagawa, Japan

Y. Takewa (✉) · E. Tatsumi
Department of Artificial Organs, National Cerebral and Cardiovascular Center Research Institute, Osaka, Japan
e-mail: takewa@ncvc.go.jp

T. Oie
Shinkan Kogyo Co., Osaka, Japan

Introduction

The homografts and replacement cardiac valves that are currently in use, including mechanical and bioprosthetic xenograft valves, are efficacious, but further development is required [1]. In the case of mechanical valves, lifetime anticoagulation therapy is required because thrombus formation around the valve can lead to insufficiency or serious embolisms. Bioprosthetic valves, on the other hand, are subject to gradual deterioration of the structure of the xenogenic tissues due to calcification [2–4]. Moreover, owing to their inability to grow, neither type of prosthetic valve is suitable for use in pediatric patients [5]. To overcome these problems, "biovalves," autologous, tri-leaflet, valved conduits, were developed using "in-body tissue architecture" technology [6]. To date, biovalves have been obtained following the encapsulation of specific molds with autologous connective tissues (collagen and fibroblasts) in the subcutaneous pouches of animals [7–11].

The formation of biovalves involves the use of acrylate or silicone molds that serve as scaffolds for the development of autologous tissues, with collagenous structure, around the mold. Formation of these devices depends upon the migration of fibroblasts from the adjacent autologous

tissues, supported by acute and chronic inflammatory reactions to the presence of the foreign mold [12, 13]. The fibroblast-induced encapsulation is regulated by growth factors secreted by activated inflammatory cells, such as macrophages, and is similar for almost all embedded biomaterial implants [14, 15]. The encapsulation occurs easily on the surface of implants in direct contact with the surrounding subcutaneous tissue [16]. However, the challenge of tissue migration to the luminal space of the implants makes filling the space extremely difficult because the natural purpose of encapsulation is to cover the foreign material. If the aperture is small, tissue migration is particularly difficult. Indeed, during the biovalve preparation process, leaflet formation, which requires tissue migration into the small apertures of the molds, is delayed in comparison with the formation of the conduit. Conduits can be completely formed within 1 month, similar to biotubes, which are similarly formed autologous tubular connective tissues for vascular grafts [6, 17, 18].

In a preliminary study, only partial leaflet formation was noticed after harvesting some biovalve molds. In this study, we examined the optimal period of subcutaneous mold implantation to produce biovalves (type VII). Using a capsule endoscope impregnated into the molds, we continuously monitored leaflet formation, in situ. To enhance leaflet formation, we assessed the effects of different biochemical approaches, using autologous fat or blood, as well as a physical approach, involving an additional opening into the mold, to promote tissue migration into the apertures.

Materials and methods

Mold preparation procedure

Six plastic parts were assembled to form the mold used to form the type VII biovalve. Five acrylate parts were prepared using a three-dimensional printer (Projet HD3000, 3D Systems, Rock Hill, SC, USA). The sixth component was made of silicone and contained the embedded capsule endoscope (EC Type 1, Olympus, Tokyo, Japan). The mold was designed such that the leaflets were formed in such a manner that they were separated from each other, in the open form.

Biovalve preparation protocol

All animal studies were performed in accordance with the "Guide for the Care and Use of Laboratory Animals" published by the US National Institutes of Health (NIH Publication No. 85-23, revised 1996) under a protocol approved by the National (Japan) Cerebral and Cardiovascular Center Research Institute Committee (No. 12002). Thirty molds were placed into the dorsal subcutaneous pouches of 10 goats (age 1–2 years; body weight 40–50 kg) under general anesthesia induced with ketamine (10 mg/kg) and maintained with isoflurane (1–3 %).

Leaflet formation within the 3 apertures was non-invasively observed using a capsule endoscope. After complete encapsulation of the molds with connective tissue, following 2 months of embedding, the implants were harvested. The biovalves, with 3 protrusions resembling the Valsalva, were obtained by removing the center part of the mold, followed by the 2 tubular parts, and the 3 hemisphere-like parts from both ends of the developed tubular tissue. Each leaflet had an area of 2.4 cm [2], and a height of 1.7 cm.

To promote leaflet formation, autologous blood was drawn by venipuncture from the goat and placed in the three apertures of the mold immediately. The clotting of autologous blood in the leaflet apertures was obtained in approximately 5 min. Autologous fat tissue was harvested from subcutaneous pouches of the goats under general anesthesia. After the fat tissue was cut into small pieces so as not to remain the fragment, the liquid-like phase of the fat tissue obtained without selection was injected into the aperture of the mold. As additional cell entrances to promote leaflet formation, the slits were designed in a part of valsalva of the mold corresponding to the tip of each leaflet formation area.

Statistics

Quantitative data are presented as means ± standard deviations.

Results

The type VII biovalve was selected as a model for the observation of the leaflet formation process. The subcutaneous biovalve formation process is shown in Fig. 1a. The mold (b) (Fig. 1b) had a rod-like shape, with three projections forming the "sinus of Valsalva"; the leaflets form inside this area in the area demarcated by the dotted lines in Fig. 1b. The part containing the embedded capsule endoscope was located at one end of the area representing the sinus of Valsalva. After subcutaneously embedding the molds, connective tissue membranes formed on the surface of the molds, surrounding the molds with connective tissue (step 1). At the same time, similar tissue migrated from the periphery of the three apertures, between the projections and the proximal conduit. Upon harvesting a mold, it was completely encapsulated with autologous connective tissue (Fig. 1c). After removal of the mold (step 2), a biovalve,

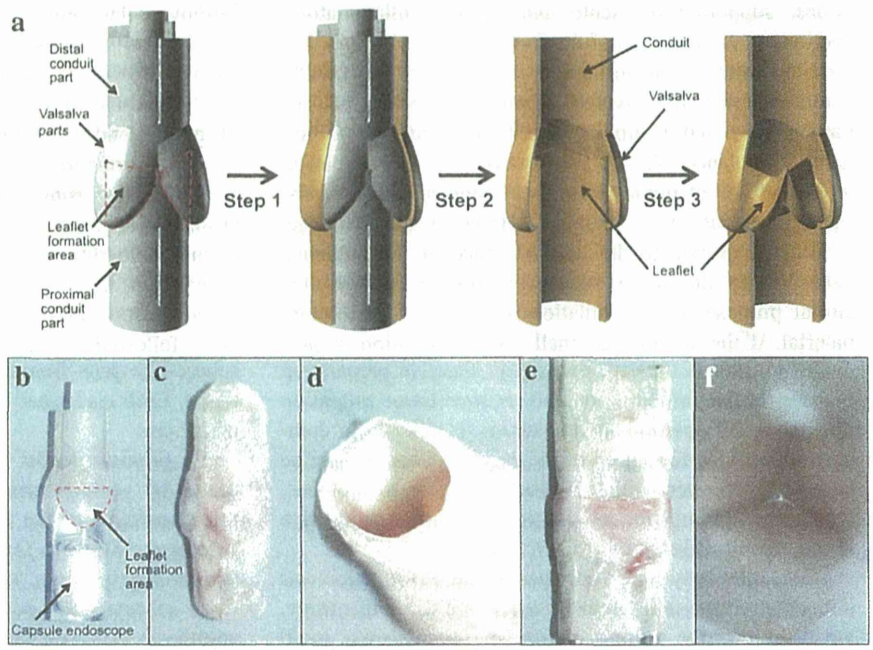

Fig. 1 **a** Schematic diagram of the formation process for Biovalve. The mold was obtained by assembling conduit and valsalva parts. The mold harvested after complete encapsulation with connective tissue (step 1). The tubular tissue with leaflet was obtained by removing the mold (step 2). Finally when air was blown through the valve, Biobalve with closed form of the leaflets was obtained (step 3). Photos of the preparation mold, impregnated with a capsule endoscope **b** before and **c** after encapsulation. Leaflet formation area indicated by *dotted red flams*. Photos of **d** circumferential cross-section and **e** luminal surface of Biovalve, and **f** the closed form of the leaflets (color figure online)

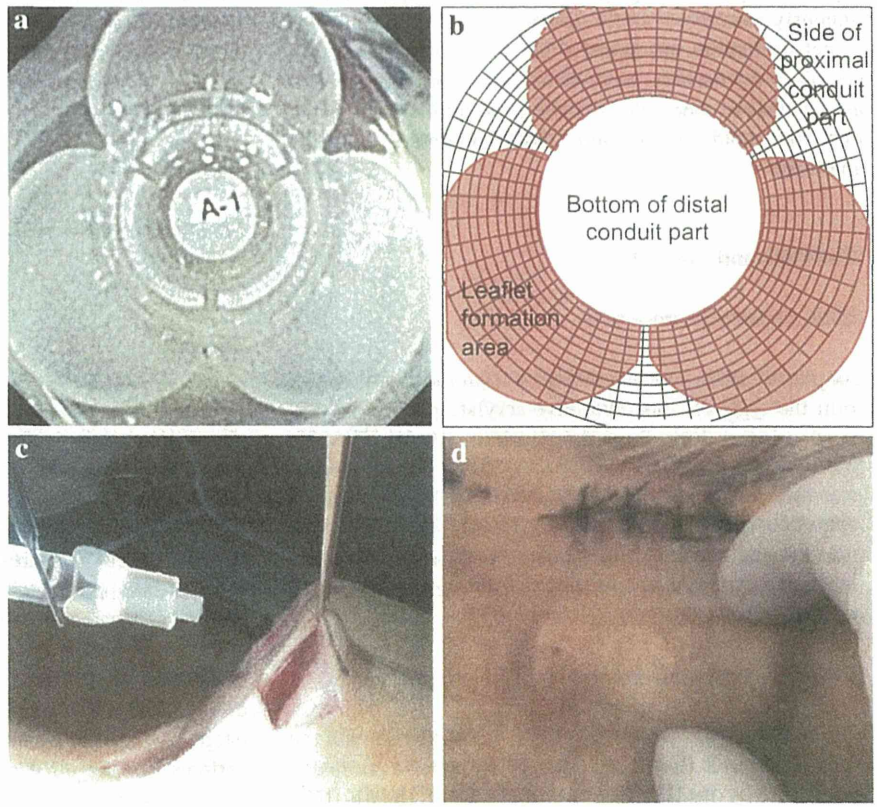

Fig. 2 Capsule endoscope view (**a**) and scheme (**b**) of the leaflet formation areas (*three red areas*). Scale of the graticule is 1 mm. **c** Embedding of the mold. **d** The mold was located approximately 3 cm from the dissection line (color figure online)

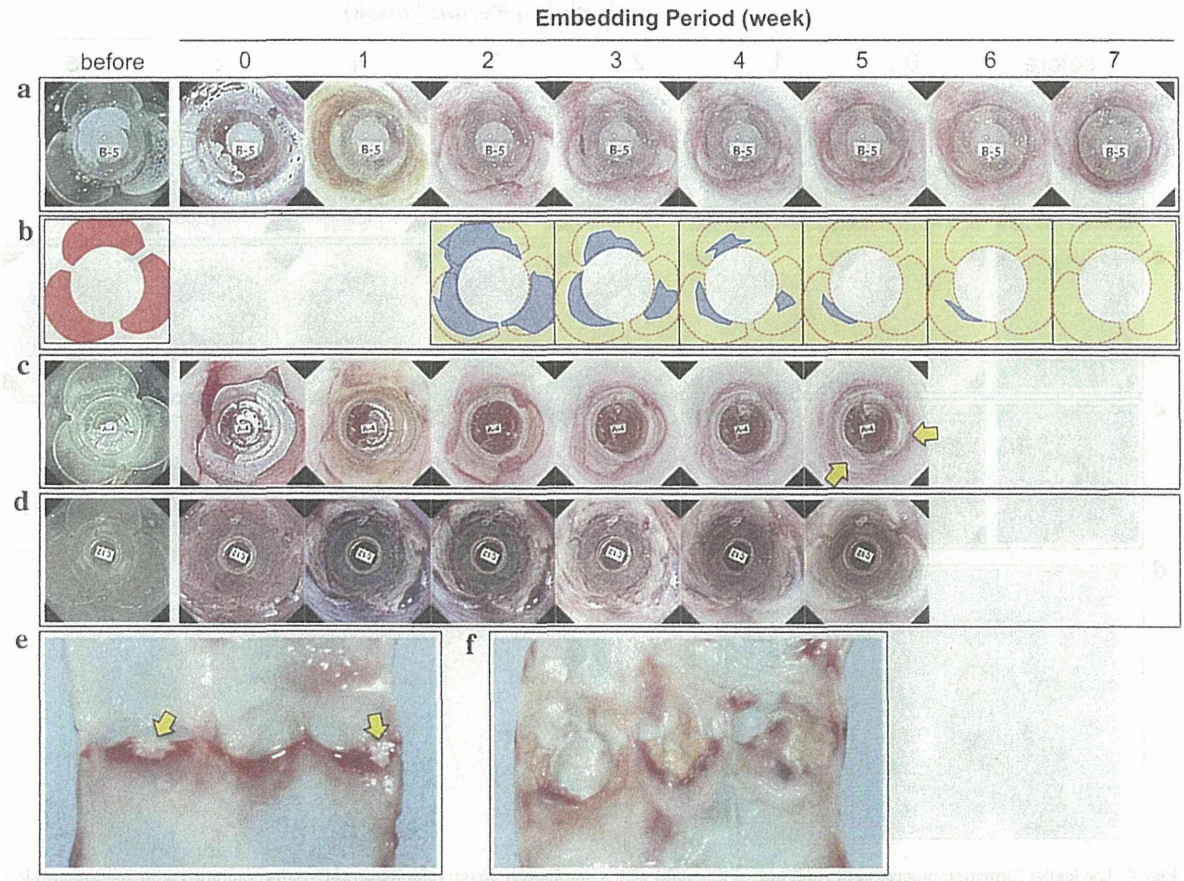

Fig. 3 Capsule endoscope view (**a**) and schematic diagram (**b**) of leaflet formation. *Red* and *blue areas* show the leaflet formed areas and remaining area for the leaflets, respectively. **c** Process of leaflet formation up to 5 weeks of implantation and **e** luminal surface of the Biovalve harvested at 5 weeks. *Yellow arrows* showed non-formation area. In post-embedding inflammation, **d** process of leaflet formation and **f** luminal surface at 5 weeks (color figure online)

with conduit tissue (Fig. 1d) connected to three leaflet membranes (Fig. 1e), was obtained. During biovalve formation, the leaflets formed in an open position. When air was blown through the valve (step 3), a biovalve with closed leaflets was obtained (Fig. 1f).

Observation of the leaflet formation process

The leaflet formation process occurred at step 1 in Fig. 1 and was non-invasively observed using the impregnated capsule endoscope. An image, acquired before implanting the mold, is shown in Fig. 2a. Three crescent-shaped leaflet formation areas (area indicated by dotted red lines in Fig. 2b), behind the three projecting parts, were clearly visualized by the endoscope at the bottom of the mold. Since the image obtained was taken with a fish eye lens, the scale was extended towards the center. After embedding, the molds were located approximately 3 cm from the dissection line (Fig. 2c, d).

Immediately after embedding, the area around the mold, including the space for the leaflet formation (red areas in Fig. 3b), was fully occupied with air (Fig. 3a). The air was gradually replaced with light yellow-colored body fluid within the first post-embedding week. After 2 weeks, the rod part of the proximal conduit (yellow areas) became the light pink, indicating the formation of connective tissue. At same time, the circumference of the crescent-shaped, leaflet formation area developed a red belt due to capillary collection. Later, the relatively white-colored area surrounding the red belt (blue areas) gradually decreased in size towards the center. After 7 weeks, the observed area was fully covered with light pink-colored connective tissue, indicating complete leaflet formation (Fig. 1e). If a mold was harvested at 5 weeks (Fig. 3c), with the remaining white-colored areas

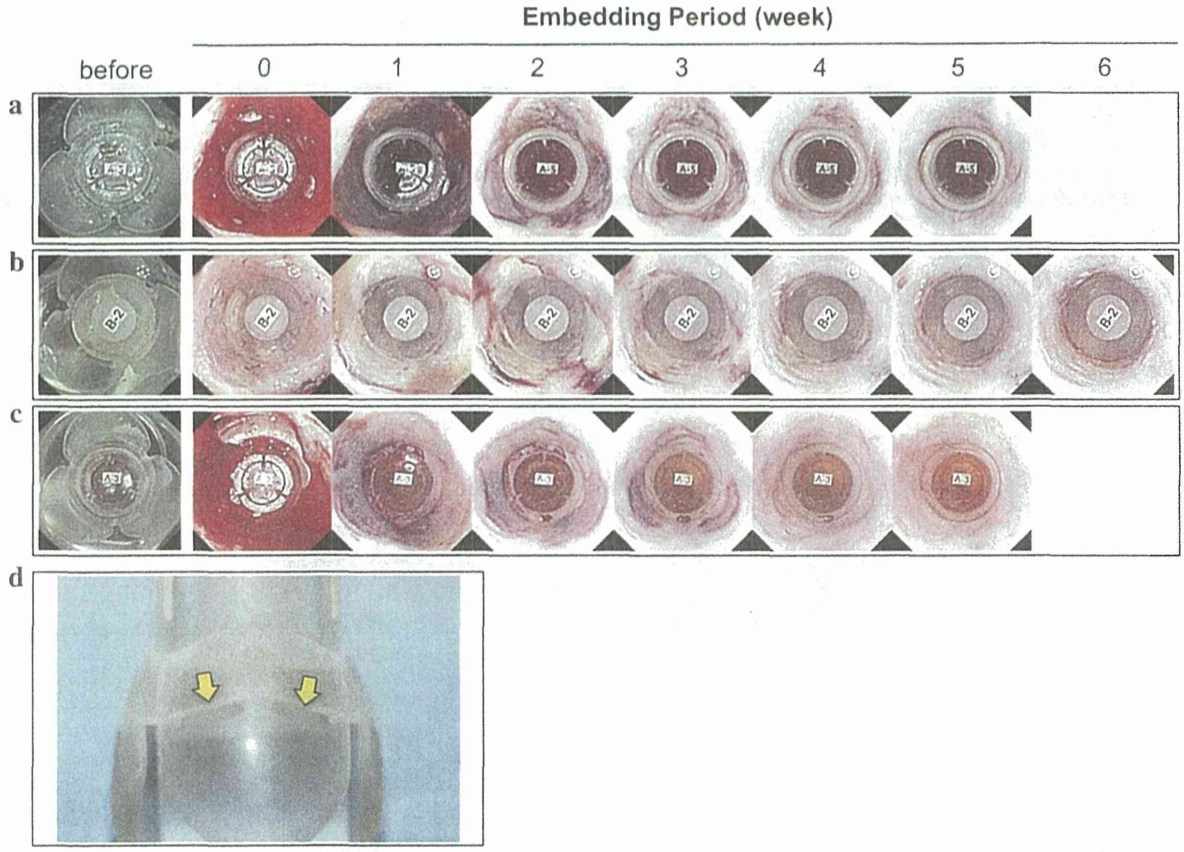

Fig. 4 The leaflet formation process at the aperture of the mold with **a** autologous blood, **b** fat tissue and **c** slits combined with autologous blood. **d** Photos of the slits in the mold as additional cell entrance. *Yellow arrows* show slits (color figure online)

indicated by the yellow arrows, the tips of the two leaflets were incompletely formed (Fig. 3e).

As post-embedding inflammation occurred, dark-colored photos were obtained (Fig. 3d), as body fluid accumulated abnormally in the subcutaneous pouch due to the inflammatory process. However, the outside of the leaflet formation area became light pink despite the persistence of the dark color in the leaflet formation area and the absence of capillary ingrowth. When harvested at 5 weeks, only the base areas of the leaflets were formed; most of the leaflet had not yet developed (Fig. 3f).

Promotion of leaflet formation

One physical and two biochemical approaches were attempted to promote leaflet formation. One approach involved the clotting of autologous blood in the leaflet apertures at the time of embedding. Immediately after embedding, the blood appeared light red, but changed to dark purple within 1 week (Fig. 4a). At 2 weeks, the development of capillary vessels appeared similar to the molds without the autologous blood clot. However, leaflet formation was complete at 5 weeks. In the original molds, without blood injections, only one mold demonstrated complete leaflet formation at 5 weeks (Fig. 5); additional biovalves were completed weekly, thereafter, with the last biovalve being completed after 12 weeks. The average time required for biovalve completion was 63.1 ± 17.1 days ($n = 11$), whereas an average of 41.1 ± 6.9 days ($n = 10$) were required when autologous blood was injected into the apertures (Fig. 5).

A similar shortening of the development period was noted in molds in which autologous fat tissue was injected into the three apertures (Fig. 4b) at the time of embedding. One week after embedding, tissue growth began; capillary vessels developed between weeks 2 and 4. The three leaflets were completely formed, across the mold, at 6 weeks. The average time required for biovalve completion was 46.7 ± 4.2 days ($n = 6$).

For the physical approach, we created slits at the tip of each leaflet formation area as additional cell entrances (Fig. 4d, yellow arrows). Upon embedding, the slits were

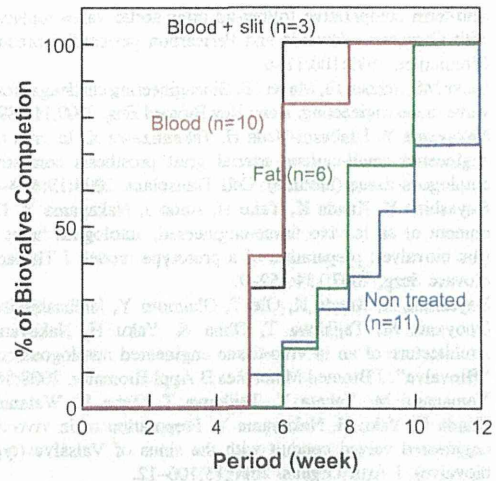

Fig. 5 The period of Biovalve completion

also injected with autologous blood. A red line developed as capillary vessels grew from both the leaflet bases and tips during a 1–2 week period. The tissue growth at the leaflet bases and tips completed within 3–4 weeks, with tissue growth gradually advancing to the central part of the leaflets and completing within 5 weeks. By combining the use of slit openings and blood injections, enhanced biovalve formation was obtained (average time to completion, 37.0 ± 2.8 days; $n = 3$).

Discussion

Biovalves were obtained by embedding molds into subcutaneous spaces in goats. However, formation of the 3 leaflets depended on the slow migration of tissue. A key problem was that we could not evaluate leaflet formation, based on external observations, making the determination of the optimal embedding period difficult. In this study, the process of leaflet formation was directly and non-invasively observed using a wireless capsule endoscope.

The overall formation process involved a foreign-body reaction, resulting from the implantation of the mold [19]. Upon implantation, protein immediately adsorbed to the mold surfaces, forming protein adsorption layers that included platelets, clots, and fibrin [15]. Afterwards, inflammatory cells, including macrophages and fibroblasts, are attracted to this layer, and the fibroblasts invade the fibrin [14]. The fibroblast invasion results in fibrinolysis and deposition of fibronectin and hyaluronan. As the early tissue matures, the fibronectin and hyaluronan are replaced with collagen types I and III, formed by the fibroblasts [12]. The collagen becomes the primary component of the biovalve leaflets [7].

The present study showed that leaflet formation began at the border of the developed capillary vessels. During wound healing, the tips of the developed capillary vessels invade the plasma-derived fibrin and fibronectin, before fibroblast migration [20]. The density of capillary vessels present in the nascent tissue gradually diminished as the collagen accumulated [21]. This series of interactions between the capillary vessels and fibroblasts conformed to the description in previous reports. Kishi et al. [22] reported that acrylic resin molds, containing velour cloth, were encapsulated within 58 days and that the new fibroblasts entered the space from between the molds. This assessment of the embedding period is important because the in vivo tissue migration process plays a key role in leaflet formation.

Two biochemical approaches and one physical approach were attempted to promote leaflet formation. In one, autologous blood was placed in the mold apertures, resulting in leaflet formation completing within 5 weeks, at the earliest. The blood contained the fibrin clot, platelets white blood cells, and various growth factors, such as vascular endothelial growth factor [23], platelet-derived growth factor (PDGF) [24], and epidermal growth factor (EGF) [25]. PDGF and EGF, in particular, are the main signals for fibroblast migration and are derived from platelets and macrophages [26–30]. The leaflet formation process, in the molds occupied by autologous blood, occurred from the base of the leaflets in the same way as in the molds occupied by air. During the second weeks after embedding, the capillary tips of blood vessels were similarly developed in the mold occupied by air and autologous blood. However, the capillary vessels were developed more quickly in the molds occupied by autologous blood thereafter. On the other hand, in the mold occupied by air, the period that neovascularity remained without tissue formation of the tip of leaflet was long. That means, during the early post-implantation phase, the current data suggest that the autologous blood affected the scaffold for fibroblast and capillary vessel migration and promoted angiogenesis.

A similar tendency for enhanced leaflet formation was noted when fat tissue was inserted into the molds. Fat tissue, including fat cells, pre-adipocytes, endothelial cells, blood vessel smooth-muscle cells, and fibroblast-like adipose precursor cells (e.g., stem cells or more committed adipose progenitors), may be an ideal scaffold for leaflet formation [31]. The fat tissue can survive and capillary vessels can grow from the adjacent environment, dependent on the required serum [32]. In addition, previous results indicated that differentiating adipose progenitors actively synthesize new extracellular matrix and are responsible for the formation of mature fat tissue [33, 34]. The current report suggests that the fat tissue retained several autologous cells, having the potential for

angiogenesis [35, 36], and promoted the angiogenesis necessary for leaflet formation in the mold. However, in this study, the eventual leaflet formation was slower than when the mold was occupied with blood. Fibroblast invasion is necessary to generate collagen, but fat tissues can survive if they receive adequate nutrients from adjacent vascularized tissue [37, 38]. As a result, the fat tissues are activated, and their replacement with collagen may be slowed.

We also created slits in the mold apertures to promote fibroblast invasion through the slits as well as from the base of the leaflets. This approach provided the shortest leaflet formation period, when combined with the use of autologous blood.

Bioprosthetic valves have superior blood compatibility and hemodynamics, compared with mechanical valves [39], but have limited durability [2–4]. Biovalve conduits have been shown to have high durability, similar to the native sinus of Valsalva and the native aorta [40–42]. The enhanced durability of these conduits may be because of their maturation after collagen replacement is complete. The durability of the leaflet tip may also be improved by the fibroblasts invading through the slits. Obtaining biovalves with adequate durability is critical for the clinical application of these bioprosthetic structures.

Conclusion

We were able to harvest the molds after an optimal development period due to the use of capsule endoscopes placed within the molds. In addition, leaflet formation was promoted by both biochemical and physical approaches. The use of wireless, capsule endoscopes solved a major problem regarding how to determine the details of the leaflet formation. This knowledge is critical to ensure that biovalve molds remain in situ long enough for complete leaflet formation to occur and ensure a high rate of harvest of functional valves.

Conflict of interest None.

References

1. Williams DF. On the mechanisms of biocompatibility. Biomaterials. 2008;29:2941–53.
2. Schoen FJ, Levy RJ. Calcification of tissue heart valve substitutes: progress toward understanding and prevention. Ann Thorac Surg. 2005;79:1072–80.
3. Manji RA, Zhu LF, Nijjar NK, Rayner DC, Korbutt GS, Churchill TA, Rajotte RV, Koshal A, Ross DB. Glutaraldehyde-fixed bioprosthetic heart valve conduits calcify and fail from xenograft rejection. Circulation. 2006;114:318–27.
4. Le Tourneau T, Savoye C, McFadden EP, Grandmougin D, Carton HF, Hennequin JL, Dubar A, Fayad G, Warembourg H. Mid-term comparative follow-up after aortic valve replacement with Carpentier-Edwards and Pericarbon pericardial prostheses. Circulation. 1999;100:11–6.
5. Sacks MS, Schoen FJ, Mayer JE. Bioengineering challenges for heart valve tissue engineering. Annu Rev Biomed Eng. 2009;11:289–313.
6. Nakayama Y, Ishibashi-Ueda H, Takamizawa K. In vivo tissue-engineered small-caliber arterial graft prosthesis consisting of autologous tissue (biotube). Cell Transplant. 2004;13:439–49.
7. Hayashida K, Kanda K, Yaku H, Ando J, Nakayama Y. Development of an in vivo tissue-engineered, autologous heart valve (the biovalve): preparation of a prototype model. J Thorac Cardiovasc Surg. 2007;134:152–9.
8. Hayashida K, Kanda K, Oie T, Okamoto Y, Ishibashi-Ueda H, Onoyama M, Tajikawa T, Ohba K, Yaku H, Nakayama Y. Architecture of an in vivo-tissue engineered autologous conduit "Biovalve". J Biomed Mater Res B Appl Biomater. 2008;86:1–8.
9. Yamanami M, Yahata Y, Tajikawa T, Ohba K, Watanabe T, Kanda K, Yaku H, Nakayama Y. Preparation of in vivo tissue-engineered valved conduit with the sinus of Valsalva (type IV biovalve). J Artif Organs. 2010;13:106–12.
10. Nakayama Y, Yahata Y, Yamanami M, Tajikawa T, Ohba K, Kanda K, Yaku H. A completely autologous valved conduit prepared in the open form of trileaflets (type VI biovalve): mold design and valve function in vitro. J Biomed Mater Res B Appl Biomater. 2011;99:135–41.
11. Mizuno T, Takewa Y, Sumikura H, Ohnuma K, Moriwaki T, Yamanami M, Oie T, Tatsumi E, Uechi M, Nakayama Y. Preparation of an autologous heart valve with a stent (stent-biovalve) using the stent eversion method. J Biomed Mater Res B Appl Biomater 2014 (in press).
12. Clark RA, Tonnesen MG, Gailit J, Cheresh DA. Transient functional expression of alphaVbeta 3 on vascular cells during wound repair. Am J Pathol. 1996;148:1407–21.
13. Thevenot PT, Baker DW, Weng H, Sun MW, Tang L. The pivotal role of fibrocytes and mast cells in mediating fibrotic reactions to biomaterials. Biomaterials. 2011;32:8394–403.
14. Song E, Ouyang N, Hörbelt M, Antus B, Wang M, Exton MS. Influence of alternatively and classically activated macrophages on fibrogenic activities of human fibroblasts. Cell Immunol. 2000;204:19–28.
15. Broughton G, Janis JE, Attinger CE. The basic science of wound healing. Plast Reconstr Surg. 2006;117(7 Suppl):S12–34.
16. Anderson JM, Rodriguez A, Chang DT. Foreign body reaction to biomaterials. Semin Immunol. 2008;20:86–100.
17. Watanabe T, Kanda K, Ishibashi-Ueda H, Yaku H, Nakayama Y. Development of biotube vascular grafts incorporating cuffs for easy implantation. J Artif Organs. 2007;10:10–5.
18. Watanabe T, Kanda K, Yamanami M, Ishibashi-Ueda H, Yaku H, Nakayama Y. Long-term animal implantation study of biotube-autologous small-caliber vascular graft fabricated by in-body tissue architecture. J Biomed Mater Res B Appl Biomater. 2011;98:120–6.
19. Luttikhuizen DT, Harmsen MC, Van Luyn MJ. Cellular and molecular dynamics in the foreign body reaction. Tissue Eng. 2006;12:1955–70.
20. Singer AJ, Clark RA. Cutaneous wound healing. N Engl J Med. 1999;2341:738–46.
21. Tonnesen MG, Feng X, Clark RA. Angiogenesis in wound healing. J Investig Dermatol Symp Proc. 2000;5:40–6.
22. Kishi A, Isoyama T, Saito I, Miura H, Nakagawa H, Kouno A, Ono T, Inoue Y, Yamaguchi S, Shi W, Abe Y, Imachi K, Noshiro M. Use of in vivo insert molding to form a jellyfish valve leaflet. Artif Organs. 2010;34:1125–31.
23. Bates DO, Hillman NJ, Williams B, Neal CR, Pocock TM. Regulation of microvascular permeability by vascular endothelial growth factors. J Anat. 2002;200:581–97.

24. Betsholtz C, Karlsson L, Lindahl P. Developmental roles of platelet-derived growth factors. Bioessays. 2001;23:494–507.
25. Bhora FY, Dunkin BJ, Batzri S, Aly HM, Bass BL, Sidawy AN, Harmon JW. Effect of growth factors on cell proliferation and epithelialization in human skin. J Surg Res. 1995;59:236–44.
26. Klinger MH, Jelkmann W. Role of blood platelets in infection and inflammation. J Interferon Cytokine Res. 2002;22:913–22.
27. Anitua E, Andia I, Ardanza B, Nurden P, Nurden AT. Autologous platelets as a source of proteins for healing and tissue regeneration. Thromb Haemost. 2004;91:4–15.
28. Diegelmann RF, Evans MC. Wound healing: an overview of acute, fibrotic and delayed healing. Front Biosci. 2004;1:283–9.
29. Li W, Fan J, Chen M, Guan S, Sawcer D, Bokoch GM, Woodley DT. Mechanism of human dermal fibroblast migration driven by type I collagen and platelet-derived growth factor-BB. Mol Biol Cell. 2004;15:294–309.
30. Butterfield TA, Best TM, Merrick MA. The dual roles of neutrophils and macrophages in inflammation: a critical balance between tissue damage and repair. J Athl Train. 2006;41:457–65.
31. De Ugarte DA, Ashjian PH, Elbarbary A, Hedrick MH. Future of fat as raw material for tissue regeneration. Ann Plast Surg. 2003;50:215–9.
32. Zhao J, Yi C, Zheng Y, Li L, Qiu X, Xia W, Su Y, Diao J, Guo S. Enhancement of fat graft survival by bone marrow-derived mesenchymal stem cell therapy. Plast Reconstr Surg. 2013;132:1149–57.
33. Nakajima I, Muroya S, Tanabe R, Chikuni K. Extracellular matrix development during differentiation into adipocytes with a unique increase in type V and VI collagen. Biol Cell. 2002;94:197–203.
34. Flynn L, Semple JL, Woodhouse KA. Decellularized placental matrices for adipose tissue engineering. J Biomed Mater Res A. 2006;79:359–69.
35. Fraser JK, Wulur I, Alfonso Z, Hedrick MH. Fat tissue: an underappreciated source of stem cells for biotechnology. Trends Biotechnol. 2006;24:150–4.
36. Cao Y. Angiogenesis modulates adipogenesis and obesity. J Clin Invest. 2007;117:2362–8.
37. Eto H, Suga H, Matsumoto D, Inoue K, Aoi N, Kato H, Araki J, Yoshimura K. Characterization of structure and cellular components of aspirated and excised adipose tissue. Plast Reconstr Surg. 2009;124:1087–97.
38. Eto H, Kato H, Suga H, Aoi N, Doi K, Kuno S, Yoshimura K. The fate of adipocytes after nonvascularized fat grafting: evidence of early death and replacement of adipocytes. Plast Reconstr Surg. 2012;129:1081–92.
39. Kidane AG, Burriesci G, Cornejo P, Dooley A, Sarkar S, Bonhoeffer P, Edirisinghe M, Seifalian AM. Current developments and future prospects for heart valve replacement therapy. J Biomed Mater Res B Appl Biomater. 2009;88:290–303.
40. Yamanami M, Yahata Y, Uechi M, Fujiwara M, Ishibashi-Ueda H, Kanda K, Watanabe T, Tajikawa T, Ohba K, Yaku H, Nakayama Y. Development of a completely autologous valved conduit with the sinus of Valsalva using in-body tissue architecture technology: a pilot study in pulmonary valve replacement in a beagle model. Circulation. 2010;122(11 Suppl):S100–6.
41. Takewa Y, Yamanami M, Kishimoto Y, Arakawa M, Kanda K, Matsui Y, Oie T, Ishibashi-Ueda H, Tajikawa T, Ohba K, Yaku H, Taenaka Y, Tatsumi E, Nakayama Y. In vivo evaluation of an in-body, tissue-engineered, completely autologous valved conduit (biovalve type VI) as an aortic valve in a goat model. J Artif Organs. 2013;16:176–84.
42. Sumikura H, Nakayama Y, Ohnuma K, Takewa Y, Tatsumi E. In vitro evaluation of a novel autologous aortic valve (Biovalve) with a pulsatile circulation circuit. Artif Organs. 2014;38:282–9.

J Artif Organs (2015) 18:48–54
DOI 10.1007/s10047-014-0796-7

ORIGINAL ARTICLE

Biomaterials

Implantation study of a tissue-engineered self-expanding aortic stent graft (bio stent graft) in a beagle model

Hidetake Kawajiri · Takeshi Mizuno · Takeshi Moriwaki · Ryosuke Iwai · Hatsue Ishibashi-Ueda · Masashi Yamanami · Keiichi Kanda · Hitoshi Yaku · Yasuhide Nakayama

Received: 19 July 2014 / Accepted: 4 October 2014 / Published online: 16 October 2014

Abstract The use of stent grafts for endovascular aortic repair has become an important treatment option for aortic aneurysms requiring surgery. This treatment has achieved excellent outcomes; however, problems like type 1 endoleaks and stent graft migration remain. Bio stent grafts (BSGs), which are self-expanding stents covered with connective tissue, were previously developed using "in-body tissue architecture" technology. We assessed their early adaptation to the aorta after transcatheter implantation in a beagle model. BSGs were prepared by subcutaneous embedding of acryl rods mounted with self-expanding nitinol stents in three beagles for 4 weeks (n = 3/dog). The BSGs were implanted as allografts into infrarenal abdominal aortas via the femoral artery of three other beagles. After 1 month of implantation, aortography revealed no stenosis or aneurysmal changes. The luminal surface of the BSGs was completely covered with neointimal tissue, including endothelialization, without any thrombus formation. The cover tissue could fuse the luminal surface of the native aorta with tight conjunctions even at both ends of the stents, resulting in complete impregnation of the strut into the reconstructed vascular wall, which is expected to prevent endoleaks and migration in clinical applications.

Keywords Endovascular aortic repair (EVAR) · Covered stents · Connective tissue · In vivo tissue engineering · Stent graft

H. Kawajiri (✉) · T. Mizuno · T. Moriwaki · R. Iwai · M. Yamanami · Y. Nakayama (✉)
Division of Medical Engineering and Materials, National Cerebral and Cardiovascular Center Research Institute, 5-7-1 Fujishiro-dai, Suita 565-8565, Japan
e-mail: kawajiricvs@yahoo.co.jp

Y. Nakayama
e-mail: ny@ncvc.go.jp

H. Kawajiri · M. Yamanami · K. Kanda · H. Yaku
Department of Cardiovascular Surgery, Kyoto Prefectural University of Medicine, Kyoto, Japan

H. Ishibashi-Ueda
Department of Pathology, National Cerebral and Cardiovascular Center, Suita, Japan

Introduction

Covered stents were initially developed as handmade fabric-covered metal stents (stent grafts) for the endovascular treatment of thoracic or abdominal aortic aneurysms and other forms of vascular disease [1, 2]. In the two decades since Parodi et al. [1] first demonstrated endovascular aortic repair (EVAR), it has become the dominant treatment modality for patients with aortic aneurysms owing to its lower postoperative mortality and morbidity rates when compared with open surgical aortic repair [3–6]. In addition, the development of mature, commercially available devices has further contributed to the popularity of EVAR.

Although significant improvements in endovascular techniques and devices have been achieved, late aortic complications such as endoleaks and stent migration still need to be addressed. Since most complications are caused by an angulated or short landing zone [7, 8] and/or the loss of adaption to late aortic remodeling [9], stent grafts that conform tightly to the native aorta are considered to be ideal.

Recently, we developed a self-expanding stent graft covered with autologous connective membranous tissues (bio stent graft; BSG) using in-body tissue architecture technology [10]. The connection between the stent and the

tissue was extremely robust. The BSGs could easily and repeatedly shrink from 9 to 2 mm with little damage. In this study, BSGs were implanted into the infrarenal abdominal aorta of beagles and their adaptation to the aorta was evaluated by histological analysis.

Materials and methods

Preparation of BSGs

The experimental animals were beagles ($n = 6$) aged 10–15 months and weighing 9.5–11.2 kg. Of the six dogs, three were used to produce BSGs, and the remaining three were subjected to stent graft implantation. All animals received care according to the Principles of Laboratory Animal Care formulated by the National Institutes of Health (Publication No. 56-23, received 1985), and the research protocol (No. 134034) was approved by the ethics committee of the National Cerebral and Cardiovascular Center Research Institute.

BSGs were prepared as described previously [10]. Briefly, the molds for the preparation of BSGs were assembled with cylindrical acryl rods (outer diameter 8.6 mm, length 40 mm), produced using a three-dimensional printer (ProJet HD 3000; 3D Systems; Rock Hill, SC, USA), and self-expanding nitinol metal stents (Luminexx: diameter 6.0 mm, length 36 mm; BARD: Karlsruhe, Germany; adjusted to an internal diameter of 9.0 mm by Piolax Medical Devices; Yokohama, Japan). The molds ($n = 9$) were embedded in triplicate into the dorsal subcutaneous pouches of three beagles. After 4 weeks, harvested BSGs were obtained by trimming the excessive connective tissue and removing the acryl rods.

Implantation of BSGs

The BSGs were compressed using a hand crimping device and placed into 10-Fr handmade deployment sheaths prior to implantation. The beagles were anesthetized via intramuscular injection of ketamine hydrochloride (20 mg/kg) maintained via intravenous injection of sodium pentobarbital (15 mg/kg). The beagles were placed in the supine position, and a longitudinal incision was made in the right groin. Then, the right femoral artery was exposed and encircled. Before the endovascular procedure, an intravenous injection of heparin (100 IU/kg) was administered. A 6-Fr sheath (Medi-kit; Tokyo, Japan) was inserted, primarily for preoperative aortography, using the Seldinger method [11]. After evaluating the anatomical features of the abdominal aorta and confirming the origins of the renal arteries by digital subtraction angiography, the 6-Fr sheath was exchanged for the 10-Fr handmade deployment sheath housing the bio stent graft. The 10-Fr deployment sheath was inserted into the abdominal aorta along a 0.035-in guide wire, and the BSG was deployed in the infrarenal abdominal aorta. The proximal edge of the graft was placed 10 mm distal to the lower (right) renal artery. After the aortography was completed, the deployment sheath was removed from the aorta. Subcutaneous injections of heparin (100 U/kg per day) were administered for 7 days to avoid acute intraluminal thrombosis following the implantation of the BSGs.

Euthanasia and tissue harvesting

Aortography was performed 1 month after the implantation of the stent. The patency and anatomical changes of the abdominal aorta were examined. Then, the beagles were euthanized and their infrarenal abdominal aortae were harvested via laparotomy. The abdominal aorta containing the stent graft was opened longitudinally to allow for macroscopic evaluation.

Histological examination

The harvested BSGs and the surrounding abdominal aorta were washed with saline and fixed with 10 % formaldehyde in a phosphate-buffered saline solution for 48 h, before being embedded in paraffin and subsequent examination by light microscopy. Circumferential sections of the middle regions of the BSGs and longitudinal sections of their edges were prepared and subjected to standard hematoxylin-eosin, Masson's trichrome, and Elastica van Gieson staining. Immunohistochemistry was performed using monoclonal antibodies against mouse α-smooth muscle actin (α-SMA; Abcam, Cambridge, UK, ab7817, 1/100 dilution).

Results

BSGs were easily and accurately implanted into the infrarenal abdominal aortae of beagles using 10 Fr deployment system (Fig. 1a, b). Post-deployment intraluminal balloon touch-up was not performed to avoid aortic injury. No malpositioning or deformity of the stent grafts was observed during implantation. Upon completion of the implantation, the lumbar arteries in the covered regions were only detected by angiography in the delayed phase, suggesting that there was no antegrade blood flow through the proximal landing zone (Fig. 1c).

Follow-up aortography, which was performed 1 month after graft implantation, demonstrated patent abdominal aortae without aneurysmal changes or migration of the BSG. In addition, no antegrade blood

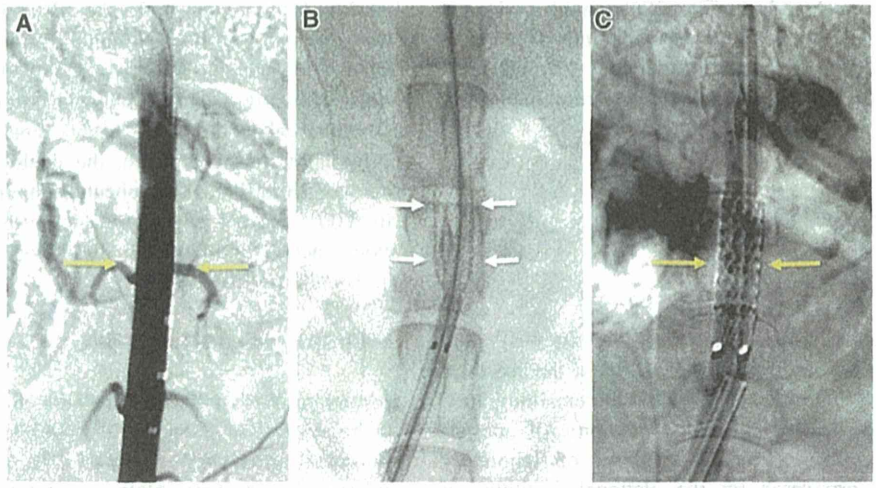

Fig. 1 **a** Aortography was performed before the deployment of the Bio stent graft (BSG) to confirm the anatomical features of the abdominal aorta. We planned to cover the lumbar arteries that are marked with *yellow arrows*. **b** The BSG (*white arrows*) was implanted precisely by pulling the outer sheath of the 10 Fr deployment system. **c** A completion angiogram after the implantation. The lumbar arteries in the covered regions were detected using angiography only in the delayed phase (*yellow arrows*), suggesting that there was no antegrade blood flow through the proximal landing zone

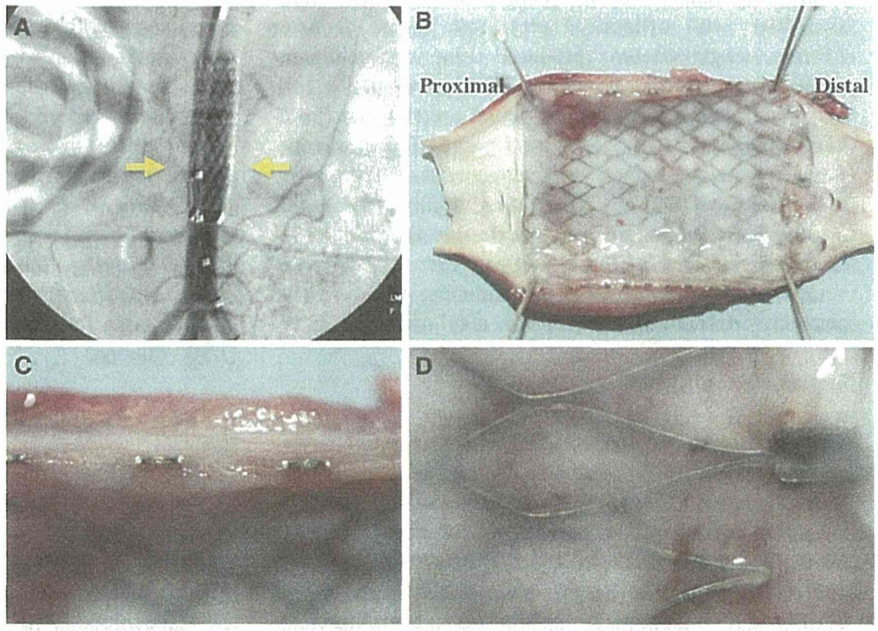

Fig. 2 **a** Follow-up aortography performed 30 days after stent implantation revealed a patent abdominal aorta without aneurysmal changes and that the BSG had not migrated. In addition, no antegrade blood flow was detected in the covered lumbar arteries (*yellow arrows*). **b** The intraluminal surface of the graft was extremely flat and no thrombi were detected. **c** The walls of the BSG had completely fused with the native aorta. **d** At the junction between the native aorta and the BSG, the autologous connective tissue that comprised the BSG had been completely covered by neointimal tissue

flow was detected in the covered lumbar arteries (Fig. 2a). After harvesting the aortae of the beagles in which the stent grafts were implanted, we injected saline from the proximal end of the resected aorta to detect type 1a endoleaks; however, no saline was extruded from the covered lumbar arteries.

When the aortic specimens were opened longitudinally, the intraluminal surface was found to be extremely flat, and no thrombi were detected (Fig. 2b). The walls of the BSGs had completely fused with the native aorta and could not be dissected (Fig. 2c). At the junction between the native aorta and the stent graft, the connective tissue membrane of

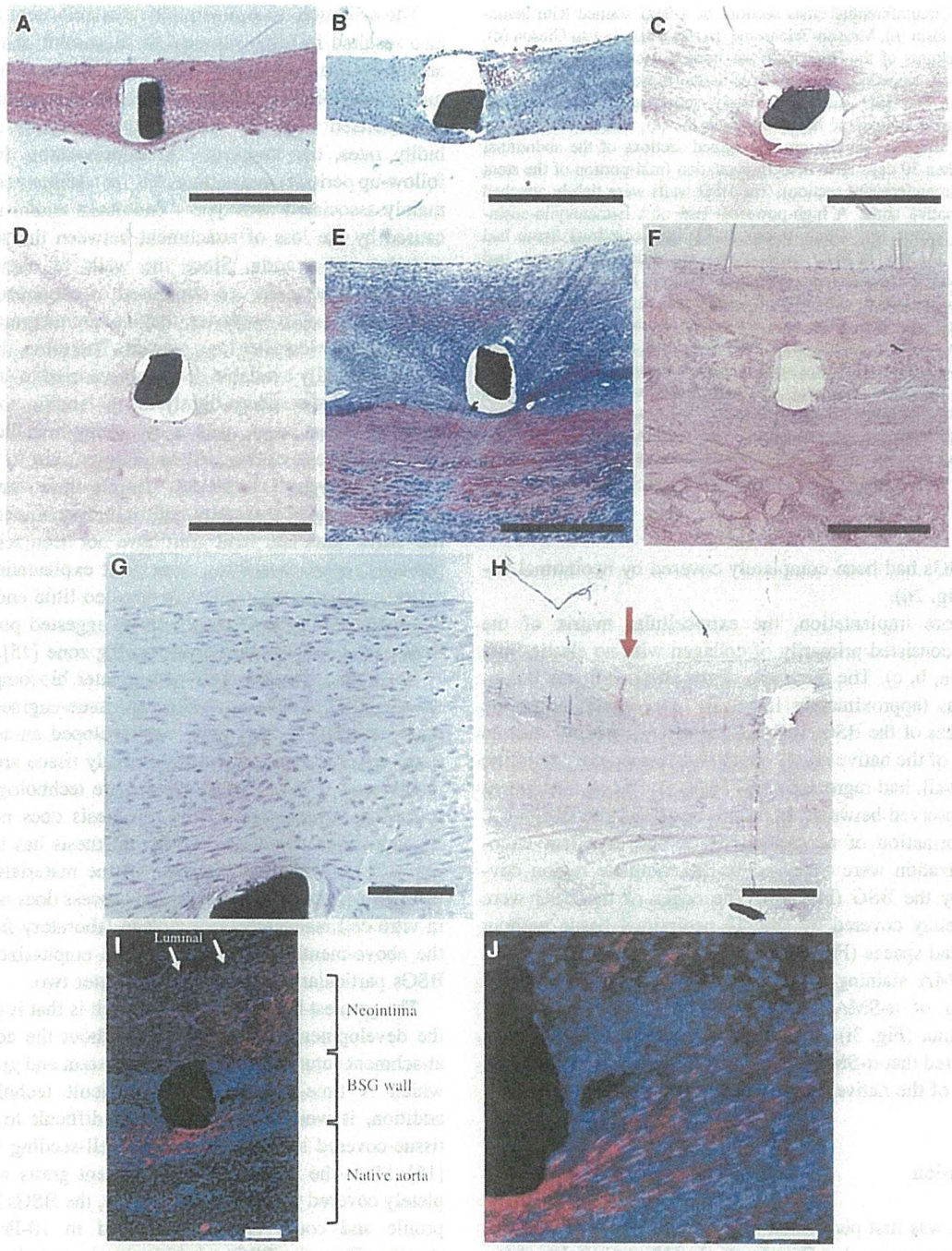
A
B
C
D
E
F
G
H
I
Luminal
Neointima
BSG wall
Native aorta
J

◀**Fig. 3** Circumferential cross sections of a BSG stained with hematoxylin-eosin (**a**), Masson-Trichrome (**b**), and Elastica van Gieson (**c**). The thickness of the BSG wall was homogeneous. The stents were completely embedded in connective tissue (thickness: approximately 150 μm). The BSG walls were mainly composed of dense collagen. Histological images of hematoxylin-eosin- (**e**), Masson-Trichrome- (**f**), and Elastica van Gieson- (**g**) stained sections of the abdominal aorta taken 30 days after BSG implantation (mid-portion of the stent graft, circumferential section). The BSG walls were tightly attached to the native aorta. A high-powered field of a hematoxylin-eosin-stained section (**g**), which demonstrated that neointimal tissue had formed on the luminal surface and an endothelial lining had developed (thickness of the neointima: 250 μm). Longitudinal section of the aorta stained with Elastica van Gieson (**h**). Smooth neointimal formation was seen at the stent graft edge (*arrow*: junction between the native aorta and stent graft). Thinning of the media was observed at the stent graft attachment site. In α-SMA staining of the sections, a number of α-SMA-positive cells were found in the BSG wall and neointima (**i**) (*arrow*: luminal surface). From examinations of high-powered fields, it was suspected that α-SMA-positive cells had migrated from the media of the native aorta to the BSG wall (**j**). *Scale bars* **a**, **b**, **c**, **d**, **e** and **f**: 500 μm; **g**: 100 μm; **h**: 1 mm; **i**: 200 μm; **j**: 100 μm

the BSGs had been completely covered by neointimal tissue (Fig. 2d).

Before implantation, the extracellular matrix of the BSGs consisted primarily of collagen with no elastic fiber (Fig. 3a, b, c). The thickness of the BSG wall was homogeneous (approximately 150 μm). After implantation, the thickness of the BSG wall was mostly unchanged, and the intima of the native aorta, which was located outside of the BSG wall, had regressed (Fig. 3d, e, f). Strong attachment was observed between the native aorta and the BSG wall. The formation of neointimal tissue and excellent endothelialization were observed in the complete region covered by the BSG (Fig. 3g). The edges of the BSG were completely covered by smooth neointimal tissue without any dead spaces (Fig. 3h).

α-SMA staining of sections of the grafts revealed a number of α-SMA-positive cells in the BSG wall and neointima (Fig. 3i). Examinations of high-powered fields suggested that α-SMA-positive cells had migrated from the media of the native aorta to the BSG wall (Fig. 3j).

Discussion

EVAR was first performed in a patient with an abdominal aortic aneurysm by Parodi et al. [1], and it has been increasingly applied to thoracic aortic aneurysms and aortic dissection as the technology has evolved [2]. Since the endovascular approach does not require thoracotomy, laparotomy, or cardiopulmonary bypass, it is less invasive than conventional open surgical repair. Thus, it has become the first-line treatment for high-risk patients, provided that their aortic anatomies are suitable [12].

The evolution of commercially available stent grafts has also resulted in improvements in successful delivery rate and long-term outcomes. However, while a number of multicenter clinical studies have demonstrated that EVAR is associated with low postoperative mortality and morbidity rates, the frequency of reintervention during the follow-up period remains high [13, 14]. Reinterventions are mainly associated with type 1 endoleaks and/or migration caused by the loss of attachment between the stent graft and the native aorta. Since the walls of commercially available stent grafts are composed of expanded polytetrafluoroethylene or polyester, they do not integrate with the native aorta, even after long periods. Therefore, developers of commercially available devices have tried to ensure that such stent grafts adhere tightly to the landing zone of the aorta in various ways, such as by putting metallic barbs at the proximal end of the graft or adding a skirt to minimize the risk of type 1 endoleaks. Despite these innovations, good stent graft conformity and tight attachment between the native aorta and stent graft have not been achieved. A previous report examining stent graft explantation due to major complications of EVAR detected little endoluminal incorporation in most cases, which suggested poor neointimal growth in the stent graft landing zone [15].

To produce a stent graft with greater biocompatibility, we attempted to develop autologous tissue-engineered stent grafts (BSGs). In this study, we developed an autologous tissue-covered stent graft using in-body tissue architecture technology. In-body tissue architecture technology has the following advantages: (1) the prosthesis does not induce immunological rejection, (2) the prosthesis has the potential to grow with the recipient, (3) the materials are biocompatible, and (4) the fabrication process does not require in vitro cell management or a clean laboratory facility. Of the above-mentioned advantages, we emphasize that our BSGs particularly benefit from the latter two.

The greatest benefit of this approach is that it allows for the development of a stent graft without the addition of attachment sutures between the metal stent and graft fabric, which is time-consuming and difficult technically. In addition, it would have been more difficult to fabricate tissue-covered stent grafts using a cell-seeding technique [16]. Since the metal stents in our stent grafts were completely covered with connective tissue, the BSGs had a low profile and could easily be housed in 10-Fr delivery sheaths. Thus, the BSGs could be implanted via a femoral approach.

As we reported previously, the elastic modulus of the walls of the BSG was approximately twice as high as that of the beagle abdominal aorta [10]. Regarding the durability of in vivo tissue-engineered cardiovascular materials, Watanabe et al. [17] described the thickness and tensile strength of an in-body tissue-engineered graft (biotube)

that was implanted into the carotid artery of a rabbit. They reported that the thickness and tensile strength of the graft were approximately twice as high at 26 months after implantation than they were before implantation. In addition, Takewa et al. [18] confirmed the in vivo durability of an in-body tissue-engineered valve (a biovalve), which was implanted into a goat as part of an apicoaortic bypass, at 2 months after its implantation. In the present study, we focused on ensuring that the BSGs developed a strong attachment to the native aorta, as we considered that such attachment would be indicative of good performance at the landing zone. Therefore, no aortic aneurysm model was used. However, based on our previous findings regarding in vivo tissue-engineered materials, the walls of our BSGs are expected to become thicker, and hence, we consider that they would be able to endure the systemic pressure that would be placed upon them in aneurysm models.

Achieving early neo-endothelialization and tight attachment to the native aorta were regarded as important goals for developing ideal aortic stent grafts. Regarding previous studies, several reports have described early results for basic fibroblast growth factor (bFGF)-releasing aortic stent grafts that were implanted into animal models [19, 20]. In these studies, the bFGF-releasing aortic stent grafts significantly accelerated the proliferation of neointimal tissue when compared with the control models. Such bFGF-releasing stent grafts might resolve some of the issues associated with EVAR; however, the walls of these stent grafts, which are made of expanded polytetrafluoroethylene, do not completely integrate with the native aortic wall. In the present study, the BSG wall completely fused with the native aorta. Furthermore, the intraluminal surface of the BSG had been entirely covered by smooth neointimal tissue within a month and no thrombosis or stenosis had occurred. Histological examinations performed after implantation of the BSGs demonstrated that the following changes had occurred: (1) α-SMA-positive cells had invaded into the BSG wall and neointima, and (2) the early formation of neointimal tissue and neo-endothelialization were observed on the luminal surfaces of the grafts. These two changes were considered to be unique to the BSGs and would not have been seen after the implantation of conventional stent grafts, the fabric portions of which are made of polyester or expanded polytetrafluoroethylene. The invasion of α-SMA-positive cells into the BSG wall, which consisted of tissue-engineered connective tissue, likely contributed to the strong attachment that was observed between the native aorta and BSG after implantation. Furthermore, the early neo-endothelialization would have influenced the creation of a smooth luminal surface at the junction between the BSG and native aorta. The above-mentioned in vivo adaptations might also have aided in the prevention of some of the complications associated with EVAR, such as type 1 endoleaks and migration.

As shown in Fig. 2f, thinning of the media was observed after BSG implantation. In addition, similar histological changes were reported in a previous animal study [21] and clinical report [9]. Such changes might be inevitable because stent grafts have to possess a strong radial force to achieve tight attachment. In the present study, the migration of α-SMA-positive cells into the BSG wall was observed; thus, we expect that aortic structures such as medial tissue containing dense elastic fibers would have developed around the stent struts in time, reinforcing the thin aortic media.

In our previous study of in vivo tissue-engineered small-caliber vascular grafts (biotubes), all grafts without anti-thrombogenic coating had become occluded within 2 weeks [22] because the original biotubes were composed of collagen fibers and fibroblasts. Thus, we established a method involving argatroban loading prior to implantation to avoid graft thrombosis during the acute phase following implantation [23]. In the present study, argatroban loading was not performed prior to implantation because the diameter of the stent graft was considered to be sufficiently large and the velocity of the blood flow through the aorta is much higher than that of the peripheral arteries. As predicted, no in-stent graft thrombosis occurred after implantation. In addition to the tremendous velocity and large caliber of the aorta, the early neo-endothelialization mentioned above might have had anti-thrombogenic effects.

Conclusion

Our developed BSGs were implanted into an animal model. After implantation into the abdominal aortae of beagles as allografts, the BSGs integrated with the native aorta within 1 month while exhibiting excellent neo-endothelialization. The findings of the present study indicate that these BSGs might solve some of the issues associated with EVAR. Further studies in aneurysm and atherosclerotic aortic models are necessary to confirm the high performance of our BSGs for clinical applications.

Acknowledgments The authors thank Mr. Yasuhiro Hoshino (Piolax) for his participation in this study.

Conflict of interest None declared.

References

1. Parodi JC, Palmaz JC, Barone HD. Transfemoral intraluminal graft implantation for abdominal aortic aneurysms. Ann Vasc Surg. 1991;5:491–9.

2. Dake MD, Miller DC, Semba CP, Mitchell RJ, Walker PJ, Liddell RP. Transluminal placement of endovascular stent-grafts for the treatment of descending thoracic aortic aneurysms. N Engl J Med. 1994;331:1729–34.
3. Knepper J, Upchurch GR. A review of clinical trials and registries in descending thoracic aortic aneurysms. Sem Vasc Surg. 2010;23:170–5.
4. Garcia-Toca M, Eskandari MK. Regulatory TEVAR clinical trials. J Vasc Surg. 2010;52:22S–5S.
5. United Kingdom EVAR Trial Investigators, Greenhalgh RM, Brown LC, Powell JT, Thompson SG, Epstein D, Sculpher MJ. Endovascular versus open repair of abdominal aortic aneurysm. N Engl J Med. 2010;362:1863–71.
6. Prinssen M, Buskens E, Blankensteijn JD, DREAM trial participants. Quality of life endovascular and open AAA repair. Results of a randomized trial. Eur J Vasc Endovasc Surg. 2004;27:121–7.
7. Torsello G, Troisi N, Donas KP, Austermann M. Evaluation of the endurant stent graft under instructions for use vs off-label conditions for endovascular aortic aneurysm repair. J Vasc Surg. 2011;54:300–6.
8. Hoshina K, Kato M, Hosaka A, Miyahara T, Mikuriya A, Ohkubo N, Miyata T. Middle-term results of endovascular aneurysm repair in Japan: does intraoerative endovascular management against the hostile aneurismal neck prevent the proximal type I endoleak? Int Angiol. 2011;30:467–73.
9. Kawajiri H, Oka K, Kanda K, Yaku H. Aneurysm formation at the both ends of an endograft associated with maladaptive aortic changes after endovascular aortic repair in a healthy patients. Interact Cardiovasc Thorac Surg. 2013;17:895–7.
10. Kawajiri H, Mizuno T, Moriwaki T, Ishibashi-Ueda H, Yamanami M, Kanda K, Yaku H, Nakayama Y. Development of tissue-engineered self-expandable aortic stent grafts (bio stent grafts) using in-body tissue architecture technology in beagles. J Biomed Mater Res B Appl Biomater. 2014 (in press).
11. Seldinger SI. Catheter replacement of the needle in percutaneous arteriography; a new technique. Acta Radiol. 1953;39:368–76.
12. JCS Joint Working Group. Guidelines for diagnosis and treatment of aortic aneurysm and aortic dissection (JCS 2011: digest version). Circ J. 2013;77:789–828.
13. Zahn R, Erbel R, Nienaber CA, Naumann FJ, Nef H, Eggebrecht H, Senges J. Endovascular aortic repair of thoracic aortic disease: early and 1-year results from a German multicenter registry. J Endovasc Ther. 2013;20:265–72.
14. Szeto WY, Desai ND, Moeller P, Moser GW, Woo EY, Fairman RM, Pochettino A, Bavaria JE. Reintervention for endograft failures after thoracic endovascular aortic repair. J Thorac Cardiovasc Surg. 2013;145:165–70.
15. Brinster CJ, Fairman RM, Woo EY, Wang GJ, Carpentier JP, Jackson BM. Late open conversion and explantation of abdominal aortic stent grafts. J Vasc Surg. 2011;54:42–7.
16. Shin'oka T, Matsumura G, Hibino N, Naito Y, Watanabe M, Konuma T, Sakamoto T, Nagatsu M, Kurosawa H. Midterm clinical result of tissue-engineered vascular autografts seeded with autologous bone marrow cells. J Thorac Cardiovasc Surg. 2005;129:1330–8.
17. Watanabe T, Kanda K, Yamanami M, Ishibashi-Ueda H, Yaku H, Nakayama Y. Long-term animal implantation study of biotube-autologous small-caliver vascular graft fabricated by in-body tissue architecture. J Biomed Mater Res B Appl Biomater. 2011;1:120–6.
18. Takewa Y, Yamanami M, Kishimoto Y, Arakawa M, Kanda K, Matsui Y, Oie T, Ishibashi-Ueda H, Tajikawa T, Ohba K, Yaku H, Taenaka Y, Tatsumi E, Nakayama Y. In vivo evaluation of an in-body, tissue-engineered, completely autologous valved conduit (biovalve typeIV) as an aortic valve in a goat model. J Artif Organs. 2013;16:176–84.
19. Kajimoto M, Shimono T, Hirano K, Miyake Y, Kato N, Imanaka-Yoshida K, Shimpo H, Miyamoto K. Basic fibroblast growth factor slow release stent graft for endovascular aortic aneurysm repair: a canine model experiment. J Vasc Surg. 2008;48:1306–14.
20. Kusanagi M, Matsui O, Sanada J, Ogi T, Takamatsu S, Zhong H, Kimura Y, Tabata Y. Hydrogel-mediated release of basic fibroblast growth factor from a stent-graft accelerates biological fixation with the aortic wall in a porcine model. J Endovasc Ther. 2007;14:785–93.
21. Bashar M, Kazui T, Terada H, Suzuki K, Washiyama N, Yamashita K, Baba S. Histological changes in canine aorta 1 year after stent-graft implantation. J Endovasc Ther. 2002;9:320–32.
22. Watanabe T, Kanda K, Ishibashi-Ueda H, Yaku H, Nakayama Y. Autologous small-caliber "biotube" vascular grafts with argatroban loading: a histomorphological examination after implantation to rabbits. J Biomed Mater Res B Appl Biomater. 2010;92:236–42.
23. Nakayama Y, Yamaoka S, Yamanami M, Fujiwara M, Uechi M, Takamizawa K, Ishibashi-Ueda H, Nakamichi M, Uchida K, Watanabe T, Kanda K, Yaku H. Water-soluble argatroban for antithrombogenic surface coating of tissue-enginnered cardiovascular tissues. J Biomed Mater Res B Appl Biomater. 2011;99:420–30.

J Artif Organs
DOI 10.1007/s10047-015-0817-1

Sutureless aortic valve replacement using a novel autologous tissue heart valve with stent (stent biovalve): proof of concept

Satoru Kishimoto · Yoshiaki Takewa · Yasuhide Nakayama · Kazuma Date · Hirohito Sumikura · Takeshi Moriwaki · Motonobu Nishimura · Eisuke Tatsumi

Received: 6 November 2014 / Accepted: 5 January 2015

Abstract We developed an autologous, trileaflet tissue valve ("biovalve") using in-body tissue architecture technology to overcome the disadvantages of current bioprosthetic valves. We designed a novel biovalve with a balloon-expandable stent: the stent biovalve (SBV). This study evaluated the technical feasibility of sutureless aortic valve replacement using the SBV in an orthotopic position, as well as the functionality of the SBV under systemic circulation, in an acute experimental goat model. Three adult goats (54.5–56.1 kg) underwent sutureless AVR under cardiopulmonary bypass (CPB). The technical feasibility and functionality of the SBVs were assessed using angiography, pressure catheterization, and two-dimensional echocardiography. The sutureless AVR was successful in all goats, and all animals could be weaned off CPB. The mean aortic cross-clamp time was 45 min. Angiogram, after weaning the animals off CPB, showed less than mild paravalvular leakage and central leakage was not detected in any of the goats. The mean peak-to-peak pressure gradient was 6.3 ± 5.0 mmHg. Epicardial two-dimensional echocardiograms showed smooth leaflet movement, including adequate closed positions with good coaptation; the open position demonstrated a large orifice area (average aortic valve area 2.4 ± 0.1 cm^2). Sutureless AVR, using SBVs, was feasible in a goat model. The early valvular functionalities of the SBV were sufficient; future long-term experiments are needed to evaluate its durability and histological regeneration potential.

Keywords Tissue engineered heart valve · Autologous tissue · Aortic valve · Aortic valve replacement · Sutureless valve

Introduction

Advances in the treatment of heart valvular disease over the past decade have resulted in an increased probability of cure and an enhanced quality of life. Bioprosthetic valves are increasingly selected as heart valve substitutes over mechanical valves because of their associated freedom from continuous anticoagulation [1, 2]. However, bioprosthetic valves have the disadvantage of being subjected to time-related structural deterioration, especially in younger people [3]. Tissue engineered heart valves (TEHVs) have the potential to overcome this limitation [4–7]. Some TEHVs have already been approved for clinical use, but only as pulmonary valves, not as aortic valves [6, 7].

Our group developed an autologous, trileaflet tissue valve ("biovalve") using in-body tissue architecture (IBTA) technology. IBTA technology is a novel

S. Kishimoto (✉) · Y. Takewa · K. Date · H. Sumikura · E. Tatsumi
Department of Artificial Organs, National Cerebral and Cardiovascular Center Research Institute, 5-7-1 Fujishiro-dai, Suita, Osaka 565-8565, Japan
e-mail: kishimoto.satoru.ri@mail.ncvc.go.jp

S. Kishimoto · M. Nishimura
Department of Organ Regeneration Surgery, University of Tottori, Tottori, Japan

Y. Nakayama (✉) · T. Moriwaki
Division of Medical Engineering and Materials, National Cerebral and Cardiovascular Center Research Institute, 5-7-1 Fujishiro-dai, Suita, Osaka 565-8565, Japan
e-mail: ny@ncvc.go.jp

Published online: 21 January 2015

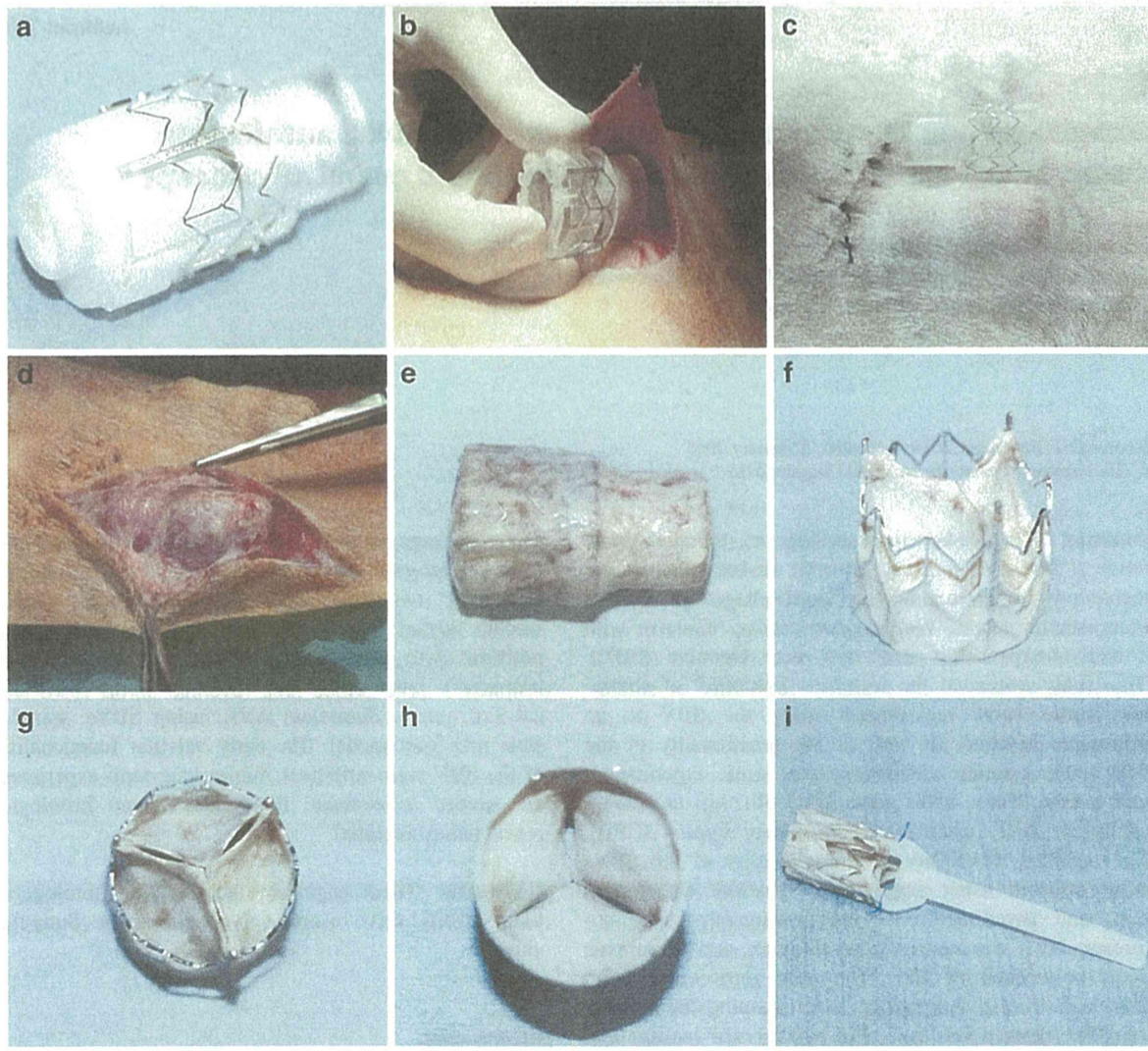

Fig. 1 The specially designed mold with stent for creating the stent biovalve (**a**). The mold is embedded in a subcutaneous pocket in a goat model (**b–c**). After 2 months, the mold, encapsulated with connective tissue, is harvested (**d**). Excess tissue is trimmed from the valve after removal of the mold (**e–i**). Crimped valve and its original holder (**i**)

regenerative medicine concept [8–12] that is based on the tissue encapsulation of foreign materials in the subcutaneous space. We believe that biovalves will become very useful aortic valve substitutes because of their good durability, even in systemic circulation in vitro and in vivo [11, 12].

In this study, we designed a biovalve with a balloon-expandable stent; the stent biovalve (SBV), for sutureless aortic valve replacement (AVR). We evaluated the technical feasibility of sutureless AVR using SBV in the orthotopic position, and the functionality of the SBV under systemic circulation in an acute experimental goat model.

Materials and methods

Experimental approval

All animals received care that was compliant with the principles of good laboratory animal care. Our institutional animal care and use committee approved the protocols (No. 13034, 14016) used in the present study.

Preparation of the stent biovalve

In consideration of the efficiency of this preliminary study, we planned to make plural valves in one goat and reserve